Chlorophyll Fluorescence Induction in Leaves of *Phaseolus vulgaris* Infected with Bean Rust (*Uromyces appendiculatus*)[1]

Richard B. Peterson* and Donald E. Aylor

Department of Biochemistry and Genetics (R.B.P.) and Department of Plant Pathology and Ecology (D.E.A.), The Connecticut Agricultural Experiment Station, 123 Huntington Street, New Haven, Connecticut 06511

To our knowledge, this report describes the first application of video imaging of Chl fluorescence to the study of light utilization in photosystem II of attached leaves of *Phaseolus vulgaris* infected with the obligate biotrophic fungus *Uromyces appendiculatus* (race 38). The video-based detection system produced a spatially resolved, quantifiable signal that was highly specific for chlorophyll fluorescence. Video images of spatial variation in the initial stage of the fluorescence induction (dark-light) transient revealed discreet regions of intense emission coinciding with centers of subsequent lesion development and accompanying chlorosis. Incipient lesions were visible by this procedure 3 d following inoculation, fully 3 to 4 d prior to visible symptoms. Fluorescence emission patterns in infected areas during the induction transient were heterogeneous with radial distance from the point of invasion and varied with the length of the time delay between re-illumination and image capture. During later ($\geq$1 min) stages of the induction transient, fluorescence emission in incipient lesions was quenched compared to surrounding tissue. These essential features of the induction transient observed in video images were also noted when individual lesions were examined using pulse modulation fluorimetry.

The capture and storage of visible light energy in leaves of higher plants is mediated by an intricate association between light-harvesting pigment-protein complexes and sequential electron transport from PSII to PSI. The efficiency of utilization of light by each of the photosystems varies in coordination with the capacity of the CO_2-fixing reactions to consume NADPH and ATP generated by the light reactions (Foyer et al., 1990). In particular, patterns of energy use in PSII with changing irradiance and other environmental conditions have been revealed by Chl fluorescence (Papageorgiou, 1975; Krause and Weis, 1991).

Light absorbed by PSII may be (a) used for primary photochemistry, (b) dissipated as heat or fluorescence, or (c) transferred to weakly fluorescent PSI. Hence, the proportion of light re-emitted as fluorescence will reflect competition among the various deactivation processes for the pool of available excitation. Illumination of leaf tissue with intense light following a period of darkness can cause fluorescence to transiently increase severalfold (Walker, 1981). The characteristic peaks and troughs in fluorescence emission following re-illumination have been studied intensively throughout the years and a nomenclature (i.e. OIDPSMT [see Abbreviations footnote] terminology [Papageorgiou, 1975]) has been adopted to describe these changes. The rapid (i.e. 1–3 s) increase in fluorescence yield from the dark level (F_O) to the peak level (F_P) is associated with reduction of the first stable electron acceptor in PSII (i.e. the quinone Q_A). Quasi-steady-state reduction of Q_A results in closure of associated PSII units to further productive photochemistry. Thus, there is an increase in deactivation of excited Chl states by means of fluorescence (Duysens and Sweers, 1963). Minor inflections (F_I and F_D) occurring on the millisecond time scale prior to F_P will not be addressed here. Reductive activation of the Calvin cycle enzymes results in sufficient linear electron transport to CO_2 to allow re-oxidation of Q_A^- within seconds of illumination, resulting in an increase in photochemical quenching of fluorescence yield (Bradbury and Baker, 1981; Quick and Horton, 1984). Establishment of a transmembrane ΔpH during electron transport can contribute to energy-dependent (i.e. nonphotochemical) quenching of fluorescence, thus reinforcing the decline in emission at this stage to a semisteady-state level (F_S). Oscillations in relative rates of utilization and production of ATP and NADPH can produce secondary fluorescence emission maxima (F_{M1}, F_{M2} ...) and minima (F_{S2}, F_{S3} ...) over a range of minutes until the terminal level (F_T) characteristic of steady-state photosynthesis is reached (Walker, 1981).

Most applications of fluorescence methodology to leaves are spatially unselective and are appropriate for conditions when local variations in emission by the leaf mesophyll are expected to be unimportant. However, video-imaging techniques have enabled study of macroscopic heterogeneity in fluorescence yield over the leaf surface associated with inhibitor treatment (Fenton and Crofts, 1990), water stress (Daley et al., 1989), and viral infestation (Balachandran et al., 1994a). Also, use of microscope optics has enabled

* Corresponding author; e-mail 72103.765@compuserve.com; fax 1-203-789-7232.

Abbreviations: F_O, F_I, F_D, F_P, F_S, F_M, and F_T, Chl fluorescence yields corresponding to the initial (nonvariable), intermediary, dip, peak, semi-steady-state, secondary maximum, and terminal levels, respectively, of the dark-light induction transient; F_{MAX}, fluorescence yield associated with complete closure of PSII centers (i.e. light plus DCMU); Q_A, primary electron accepting plastoquinone of PSII.

selective examination of light utilization by guard cells in situ (Cardon and Berry, 1992).

To our knowledge, this is the first study to report changes in the dark-light fluorescence induction transient in leaves of *Phaseolus vulgaris* infected with the fungus causing "bean rust" (*Uromyces appendiculatus*). Early stages of the obligate biotrophic (parasitic) association between *U. appendiculatus* and the susceptible host bean leaf tissue are characterized by minimal host cell damage and an absence of necrotization of lesions. Fungal spores germinate on the leaf surface and the fungus penetrates nearby stomatal openings to access the mesophyll tissue (Gold and Mendgen, 1984). The fungus breaches the cell walls of host cells after localized release of hydrolytic enzymes. These events are completed within 3 d of inoculation. Specialized fungal structures facilitate nutrient transfer from the mesophyll cell cytoplasm to the fungus (Hardham, 1992; Mendgen and Deising, 1993). Studies of carbon uptake and utilization indicate that a loss in photosynthetic capacity can occur with onset of sporulation, probably because of loss of Chl (Livne, 1964). Also, fungal metabolism constitutes a significant sink for ^{14}C-labeled photosynthate in infected leaves, resulting in changes in translocation patterns throughout the plant (Livne and Daly, 1966).

The purposes of this work were to (a) test the feasibility of video imaging as a tool for study of the development of disease, (b) compare patterns of fluorescence changes with appearance of visible features in lesions over time, and (c) assess the extent of effects of infection on photosynthesis in green tissue surrounding incipient lesions.

MATERIALS AND METHODS

Plant Material

Seeds of *Phaseolus vulgaris* (var Bush Blue Lake 47) were germinated and grown in a commercial potting soil mixture and supplemented weekly with nutrients. Growth chamber conditions were 12 h of light:12 h of dark with corresponding day:night temperatures of 22 and 17.5°C. Light was provided by a combination of cool-white fluorescent and incandescent lamps and maintained, unless indicated otherwise, at 400 μmol photons m^{-2} s^{-1}. Trifoliate leaves of 2- to 3-week-old plants were inoculated. Spores of *Uromyces appendiculatus* (race 38) were collected from mature lesions of rust-infected bean plants. A quantity of spores was added to distilled H_2O and Tween 20 was introduced until the spores were suspended uniformly. Leaves were inoculated with the spore suspension using an atomizer. Plants were then placed in a dew chamber for 24 h and subsequently transferred to the growth chamber (d 1 postinoculation). Mean lesion densities ranged from 1 to 3 lesions cm^{-2}.

A chimeric variety of *Nicotiana sylvestris* possessing sectors low in Chl (i.e. Chl$^-$) content was grown in soil in a greenhouse.

Video Imaging of Chl Fluorescence and Related Procedures

Wide-band blue light (50 μmol photons m^{-2} s^{-1}), provided by passage of white light produced by a tungsten-

halogen source through a colored glass filter (Schott [Duryea, PA] BG28, 3 mm thick), was used to excite fluorescence in attached bean leaves at room temperature (25°C). A flexible fiberoptic fitted with a collimating lens was used to direct the excitation light to the leaf surface at an incident angle of approximately 75°. A red cut-on filter (Schott RG665, 3 mm thick) was mounted in front of the camera lens to block transmission of reflected excitation light. Transmitted light was collected by a Computar (Tokyo, Japan) zoom lens (model LMZ45C5, focal length of 18–108 mm) mounted on a black and white CCD-500B low light camera (Recognition Technologies, Inc., Holliston, MA). The camera (sensitive to wavelengths of up to 1100 nm) was mounted perpendicular to the leaf surface. The automatic gain control of the camera was disabled at all times, although the sensitivity could be varied manually. A 1.0-cm^2 area of leaf surface was imaged. The video signal was sent to an MV1 Frame/Line Grabber board (Keithley Metrabyte Corp., Taunton, MA) installed in a Zenith 386SX computer. The digital image was composed of an array of 512 × 512 pixels. Each pixel displayed gray levels with 8-bit resolution so that pixel intensity ranged from 0 (black) to 255 (white). Acquisition time for capture of a frame by the MV1 board was 33 ms. A maximal estimate of the lag in camera response was obtained by capturing an image of a digital timer display incrementing in units of 0.1 s. This approach indicated that the lag in camera response was ≤67 ms, which is short compared to the time scale of changes in fluorescence emission under study here. System software overhead introduced a 0.6-s delay between the command to capture a frame and actual acquisition. The monochrome video output was displayed on a Sony Trinitron television monitor. Image-processing software consisted of the RMAC (version 1.10) package supplied by Recognition Technology, Inc. Median gray level values for each pixel were computed on the basis of a 3- × 3-pixel neighborhood to reduce random noise. Image files were converted into tagged image file format, loaded into Microsoft PowerPoint 3.0, and photographed from an SVGA monitor (640 × 480 pixels) using Kodak Plus-X black and white film (ASA 125).

Steady-state fluorescence images were acquired after 3 to 5 min of illumination in the blue light when it was confirmed that the emission intensity was constant. For fluorescence induction transients, leaf material was darkened for 5 min by placement of a size 10.5 black rubber stopper over all but a small portion of the field of view. At the end of the dark period the stopper was removed and a manual command was given to the system to acquire a frame. The total delay between re-illumination and frame capture was about 0.6 to 1.0 s. Images were also acquired for material illuminated with white light as a means of recording visual changes in leaf condition.

Separate measurements were performed to establish the dependence of gray level on light input into the video camera and to provide for comparisons of Chl fluorescence emission by leaves. White light was used to uniformly illuminate a 1.0-cm^2 area of a filter paper disc and the mean gray level was recorded as the irradiance was varied for a

fixed system sensitivity using neutral density filters. Light entry into the camera could also be varied (stepwise by a factor of 2) using the lens aperture. Mean gray level was based on a signal obtained for a contiguous 18 × 18 block of pixels.

Mean gray level increased in fixed proportion with increasing incident light intensity for values of the former ≤150 but the relationship was nonlinear for gray level >150 (Fig. 1A). The nonlinearity at high irradiance is due to compensation incorporated into the camera electronics to protect from overload. The camera lens aperture was adjusted to avoid the higher gray levels where the effects of this compensation were greatest. Failure of the linear portion of the plot in Figure 1 to extrapolate to the origin was due to an electronic offset applied to the analog video input signal at the level of the MV1 board prior to digital processing. Separate measurements (Fig. 1B) were performed to define the dependence of mean gray level and relative radiant energy input at very low values of the latter (<5.0). Although the spectral composition of red light admitted into the detection system arising from backscattered white light and Chl fluorescence will likely differ, each remains fixed under the conditions used here. Furthermore, fluorescence emission intensity is directly proportional to the equivalent relative radiant energy input of white light, which when substituted into the appropriate regression equation (Fig. 1) yields the observed mean gray level. This provides a basis for assessment of the degree of specificity of the system for Chl fluorescence.

Pulse-Modulated Fluorescence Yield Measurements

Spatially unresolved fluorescence yield measurements were made with a system using a weak, modulated measuring beam of red light (685 nm) to excite fluorescence (H. Walz, Effeltrich, Germany). This system responds only to modulated fluorescence emission for wavelengths ≥700 nm (Schreiber et al., 1986). Individual lesions were examined with this system by masking the tip of the fiberoptic probe carrying the measuring beam and nonmodulated exciting light with Al foil pierced to form a 2-mm-diameter hole to exclude signal from surrounding tissue.

Miscellaneous

Pigment analysis of 97% acetone extracts of leaf tissue samples was conducted by HPLC using a 0.46- × 25-cm reverse-phase Spherisorb column eluted with acetonitrile: H_2O:ethyl acetate (22:1:6). Tissue was frozen in liquid N_2 prior to extraction. This system separated the major leaf xanthophylls (i.e. lutein, zeaxanthin, violaxanthin, and neoxanthin). Inhibition of PSI-dependent re-oxidation of Q_A was accomplished by floating 1.2-cm-diameter leaf discs overnight on 100 μM DCMU in 1% (v/v) ethanol. Control discs were floated on 1% (v/v) ethanol. Photon flux rates were measured with a Li-Cor (Lincoln, NE) LI-190SB quantum sensor.

RESULTS

General Aspects of Video Imaging of Chl Fluorescence in Leaves

When illuminated with blue light, signals obtained from images of white filter paper were very low but detectable (Fig. 1, inset). At the same system sensitivity, DCMU-treated normal tobacco leaf tissue produced the maximum fluorescence emission and this was 5-fold higher than for the identical control material. Low levels of fluorescence were detected in leaf tissue deficient in Chl. Enhancement of this fluorescence by DCMU indicates, nevertheless, that a photochemically functional PSII was present in the mutant tissue.
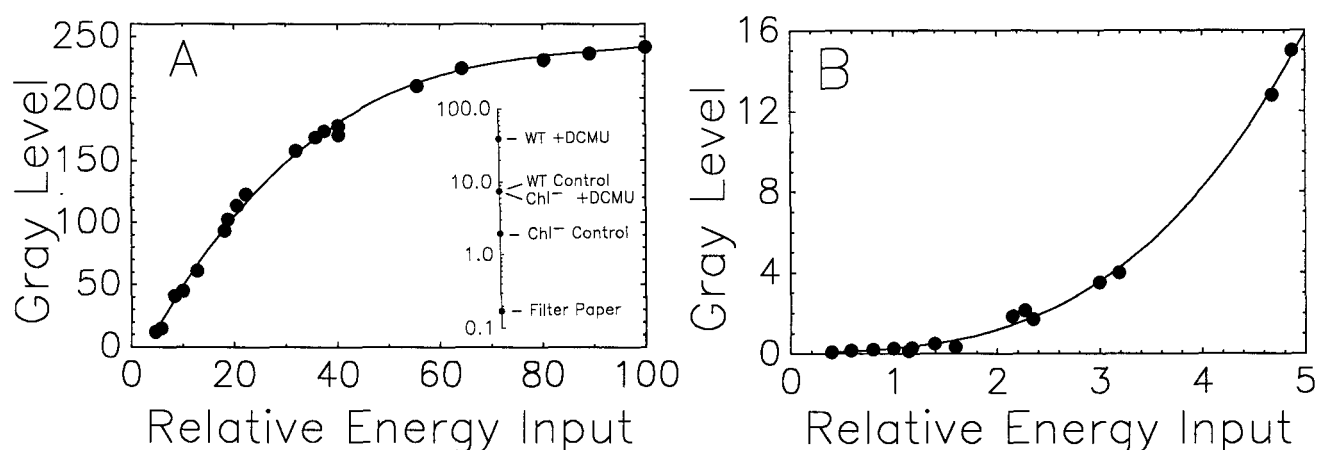

Figure 1. Quantitative relationship between relative radiant energy input into the camera and mean gray level for the video-imaging system. The maximum incident light level used (corresponding to a mean gray level of 241.4) was arbitrarily assigned a value of 100. A and B, The system response for ranges of variation in relative energy input of 5 to 100 and 0 to 5, respectively. The solid lines are third-order polynomial fits to the data (coefficients of determination = 0.997). A, inset, The corrected system response obtained for various materials illuminated with blue light. The inset scale represents the corrected magnitude of light emission expressed in terms of the equivalent energy input of white light into the camera obtained from the observed gray level and the fitted responses shown in the main figure. Chl⁻ refers to Chl-deficient tissue obtained from a chimeric variety of *Nicotiana sylvestris*. See "Materials and Methods" for further details. WT, Wild type.
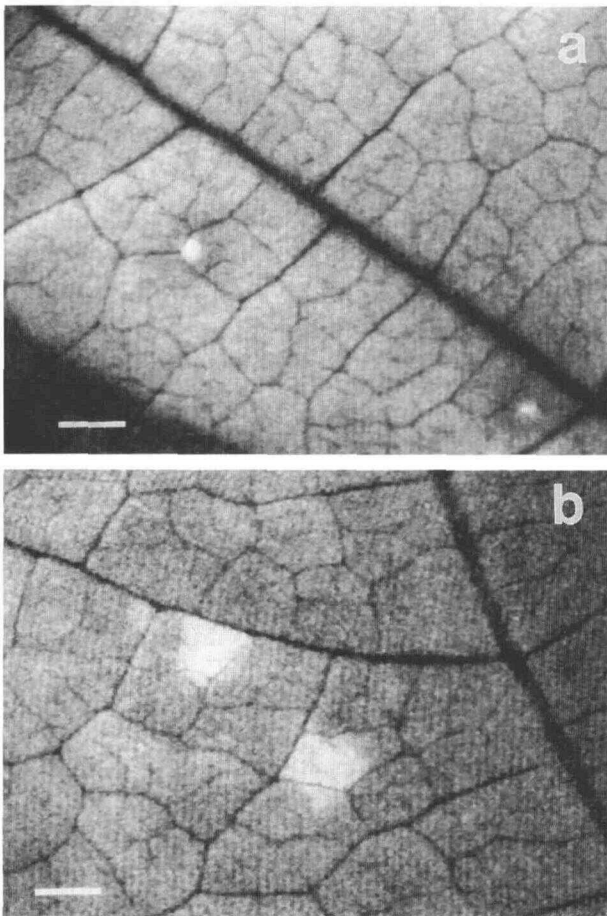
Figure 2. Representative images of Chl fluorescence obtained 0.6 to 1.0 s after re-illumination following 5 min of darkness for two leaves of bean 3 d after inoculation with bean rust spores. Note the dark zones encircling the highly fluorescent centers of the lesions in a. Bars on these images indicate 1.0 mm. Darkened area in the lower left of a was not subjected to the prior dark period and therefore represents F_T.

A direct quantitative comparison of the video imaging and Walz systems was conducted at low levels of photosynthetically active light using leaf discs from bean. Fluorescence intensity was first measured in blue light (50 μmol photons m^{-2} s^{-1}) in replicate discs in the presence and absence of DCMU using video imaging. Mean pixel gray levels were adjusted to compensate for the nonlinearity of our system (Fig. 1). Next, fluorescence yield was measured in white light (73 μmol photons m^{-2} s^{-1}) for the same discs using the Walz system. If we assume that the F_{MAX} was that measured in the presence of DCMU (Quick and Horton, 1984) and F_T was given by the signal in the absence of DCMU, then suppression of fluorescence associated with uninhibited PSII was $(F_{MAX} - F_T)/F_{MAX}$. The $(F_{MAX} - F_T)/F_{MAX}$ value determined by the video-imaging technique was 0.812 (mean of two samples). The respective mean based on measurements with the Walz system was very similar (i.e. 0.792).

Fluorescence Induction and Bean Rust Infection

Examples of enhanced fluorescence emission associated with incipient lesions observed 3 d after inoculation of bean leaves are shown in Figure 2. There was no indication of lesion development in the areas shown when either steady-state fluorescence (F_T) or reflected light was examined. Effects of infection on fluorescence prior to this time were not detected under the conditions used. In some images (i.e. Fig. 2a) the compact region of high fluorescence was surrounded by a zone of diminished emission relative to that of uninfected tissue. As little as 1 min of predarkening was sufficient to visualize incipient lesions during the subsequent fluorescence induction transient.

By d 7 postinoculation incipient lesions could be recognized visually as small protuberances on the leaf surface caused by extension of the epidermal cell layer due to growth of the fungus. At this stage the highly fluorescent central region of the lesions had expanded to a diameter of approximately 2 mm (Fig. 3a). Representative time courses of the initial phase of fluorescence induction shown in Figure 3b indicate that fluorescence emission levels reached at 0.6 to 1.0 s after restoration of excitation are positively related to the respective maximum (i.e. F_P) levels. With respect to the full course of fluorescence induction, lesions exhibited a higher F_P level and a depressed M peak compared to uninfected tissue.
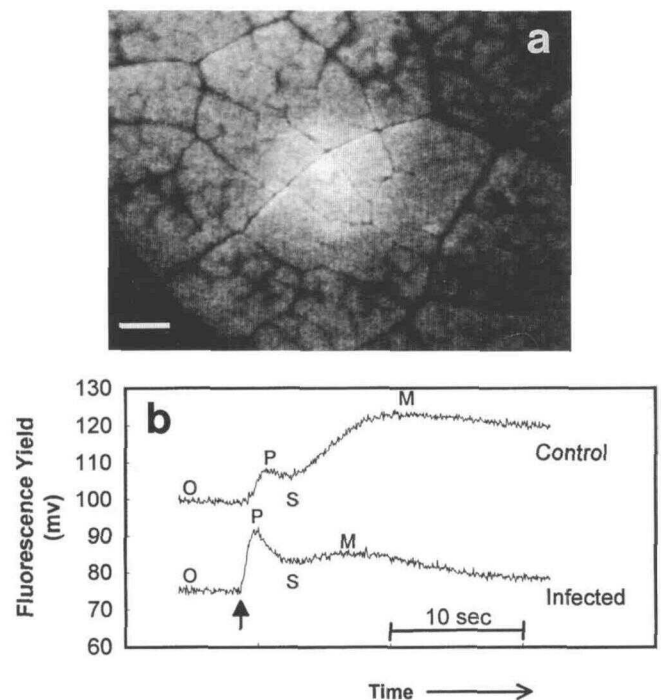

Figure 3. a, A representative image of F_P for a lesion 7 d after inoculation. b, Typical time courses of fluorescence during the dark-light induction transient (5 min of dark preincubation) using the Walz pulse modulation system for selected 2-mm-diameter areas on the leaf shown in a. Characteristic inflection points in the induction transient are labeled as O, P, S, and M corresponding to F_O, F_P, F_S, and F_M, respectively, as explained in the text. Recording was stopped before the terminal (F_T) level was attained in these experiments.

Highlights of the time course of lesion development from the perspectives of visible reflective properties and associated effects on F_T and F_P are shown in Figures 4 through 6. First, visual evidence of lesion development was absent at d 4 (Fig. 4c) but did become barely perceptible in images of reflected light at d 6 after inoculation (not shown). Following d 6 centers of infection became increasingly apparent as small white areas (flecks) in images of reflected light (Fig. 5c). Flecking preceded appearance of readily recognizable, opaque spore masses by d 10 (Fig. 6c) and severe chlorosis at d 16 (Fig. 6f). Second, steady-state fluorescence emission (F_T) remained essentially featureless through d 7 (Figs. 4a and 5a). This suggests that flecking occurring during this period represents an optical effect, arising possibly from separation of the epidermis and the mesophyll tissue rather than chlorosis. Following d 7 postinoculation loss of Chl around centers of infection became readily apparent as dark areas in images of steady-state fluorescence emission (Fig. 6, a and d). Third, the initial stage of the fluorescence induction transient showed dramatic changes during the time depicted in Figures 4 through 6. At d 4 compact areas of high fluorescence yield coincided with the centers of lesion development (Fig. 4b). These highly fluorescent ar-

eas were encircled by tissue with a lower fluorescence yield than the relatively homogeneous background emission associated with normal, uninfected lamina (see also Fig. 3). At d 6 the central highly fluorescent areas had grown in size and were surrounded by a faint ring of fluorescence (Fig. 4d). At this time, areas of low emission were interspersed among the fluorescent centers, suggesting a radial advance of characteristics observed on d 4 to an extent that an overlapping of effects of neighboring lesions occurred. By d 7 the outward growth of the zones possessing high F_P had progressed to the extent that features originating with specific lesions could no longer be resolved (Fig. 5b). Spatial variation in F_P around sporulating lesions was likely compounded by effects of chloroplast disintegration (as manifested by loss of Chl) on fluorescence induction phenomena. Figure 6b shows little variation in F_P at d 10 that could be attributed to infection. Nevertheless, intense levels of F_P were observed surrounding mature lesions on d 16 (Fig. 6e), indicating that a spread of effects on photosynthesis from lesions into adjacent green tissue can occur even at a late stage of lesion development. Direct measurement of mean lesion size based on diameter of the chlorotic zone at d 24 yielded a value of 2.85 mm (SD = 0.23).
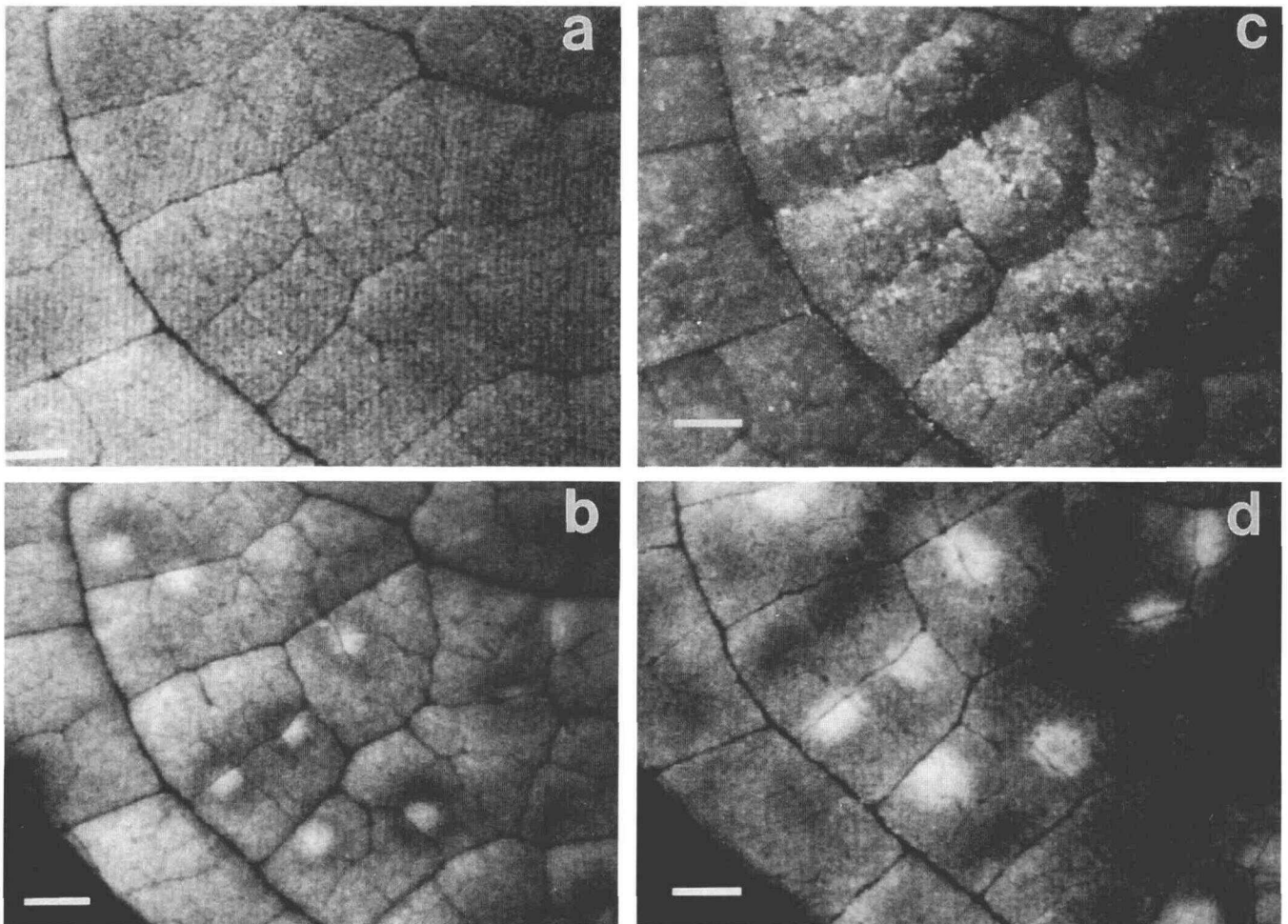

Figure 4. Images of steady-state fluorescence (a), emission at 0.6 to 1.0 s following re-illumination preceded by 5 min of darkness (b), and reflected light (c) for the same bean leaf 4 d postinoculation. d, The same as b except 6 d after inoculation.
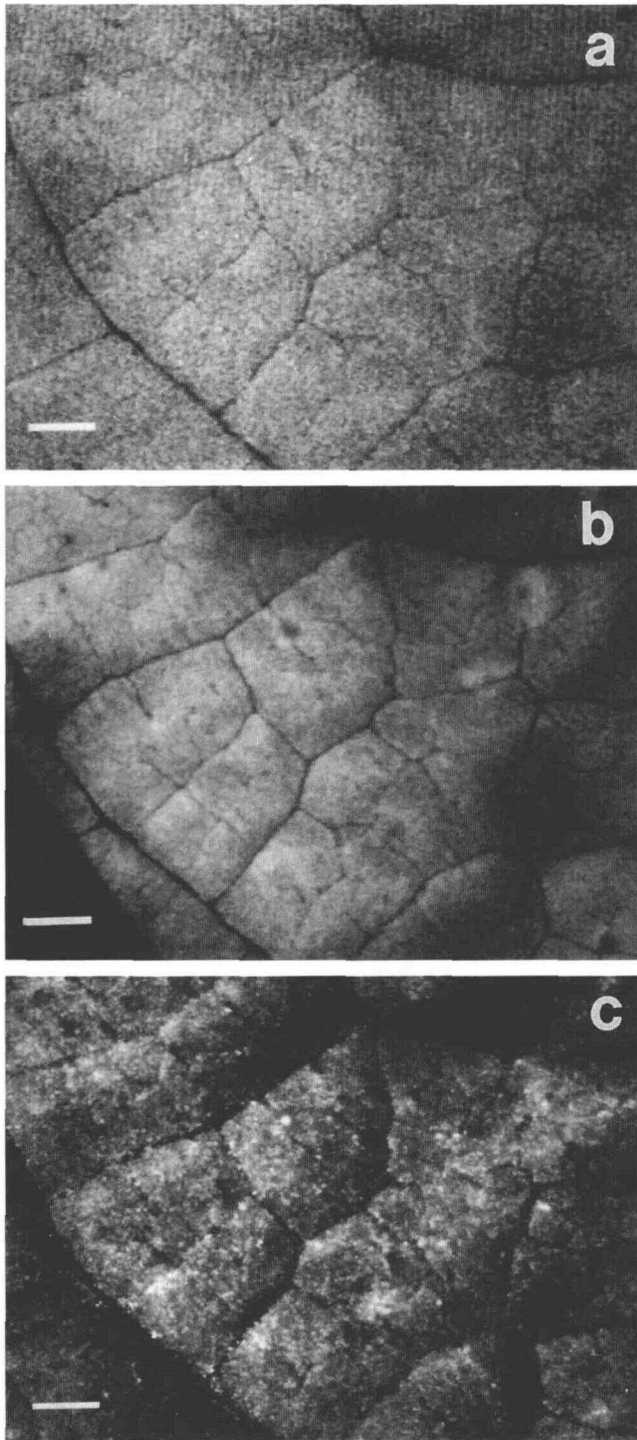
Figure 5. Images of steady-state fluorescence (a), emission at 0.6 to 1.0 s following re-illumination preceded by 5 min of darkness (b), and reflected light (c) for the leaf of Figure 4 at d 7 after inoculation. Note the appearance of white flecks (approximately 0.1 mm) near the center of the image. These constitute the first visible signs of infection.

Effects of fungal infection on fluorescence induction appeared to reach a climax on d 7 after inoculation even though loss of Chl was minimal (Fig. 5b). Fluorescence induction in infected tissue was examined further at this stage by introduction of delays between re-illumination and capture of a video image. Figure 7a shows that adding a 3-s delay results in an image with distinct concentric rings of varying fluorescence yield. Comparison of Figures 5b and 7a indicates that, although specific neighboring regions around a lesion may possess similar values of F_P, the kinetics of decline in fluorescence from F_P in these regions can vary considerably. Introduction of a 60-s delay between re-illumination and frame capture results in a substantially different image in that the lesions appear considerably darker than the surrounding tissue (cf. Figs. 5b and 7b). This indicates that fluorescence quenching processes are enhanced in infected leaf tissue during this phase of the induction transient.

We are aware of the considerable evidence for the role of xanthophylls, notably zeaxanthin, in regulation of light utilization in green tissues (Demmig-Adams and Adams, 1992). It was considered possible that infection-dependent changes in fluorescence could be associated with operation of the xanthophyll cycle. Preliminary examinations of acetone extracts of control and infected (7 d) leaf tissue grown at 200 μmol photons m^{-2} s^{-1} in air were conducted by HPLC. Zeaxanthin levels were barely detectable and not significantly different in control and infected tissues. Levels of other leaf xanthophylls were unaffected as well.

DISCUSSION

The results presented here confirm that methodology for spatial resolution of light emission by leaf material based on video imaging is specific for Chl fluorescence. About 80% of the total emission was variable as confirmed by parallel determinations using a conventional pulse-modulated measurement technique. This is consistent with prior reports for green leaf tissue (Krause and Weis, 1991). High selectivity for Chl fluorescence (Fig. 1, inset) indicates a low degree of spectral overlap between the blue excitation light and the detection system. In the case of bean rust infection, imaging of Chl fluorescence shows that distinct alterations in light utilization (a) constitute an early host response to infection that precedes visual symptoms by 3 to 4 d, (b) predict, in terms of physical extent, by d 6 or 7 postinoculation subsequent chlorosis characteristic of the end stage of the disease, and (c) occur with interacting spatial and temporal heterogeneity.

Because of the high degree of integration among primary photochemistry, electron transport, and carbon metabolism, inhibition of any component reaction will result in feedback regulation of PSII and a reduction in the efficiency of light utilization for photosynthesis. Hence, Chl fluorescence usually does not provide precise information concerning the stress mechanism (Owens, 1995). Nevertheless, changes in fluorescence yield frequently precede visible indicators of stress and can provide quantitative information about overall changes in light utilization efficiency with stress intensity and duration. Early systems for spatial
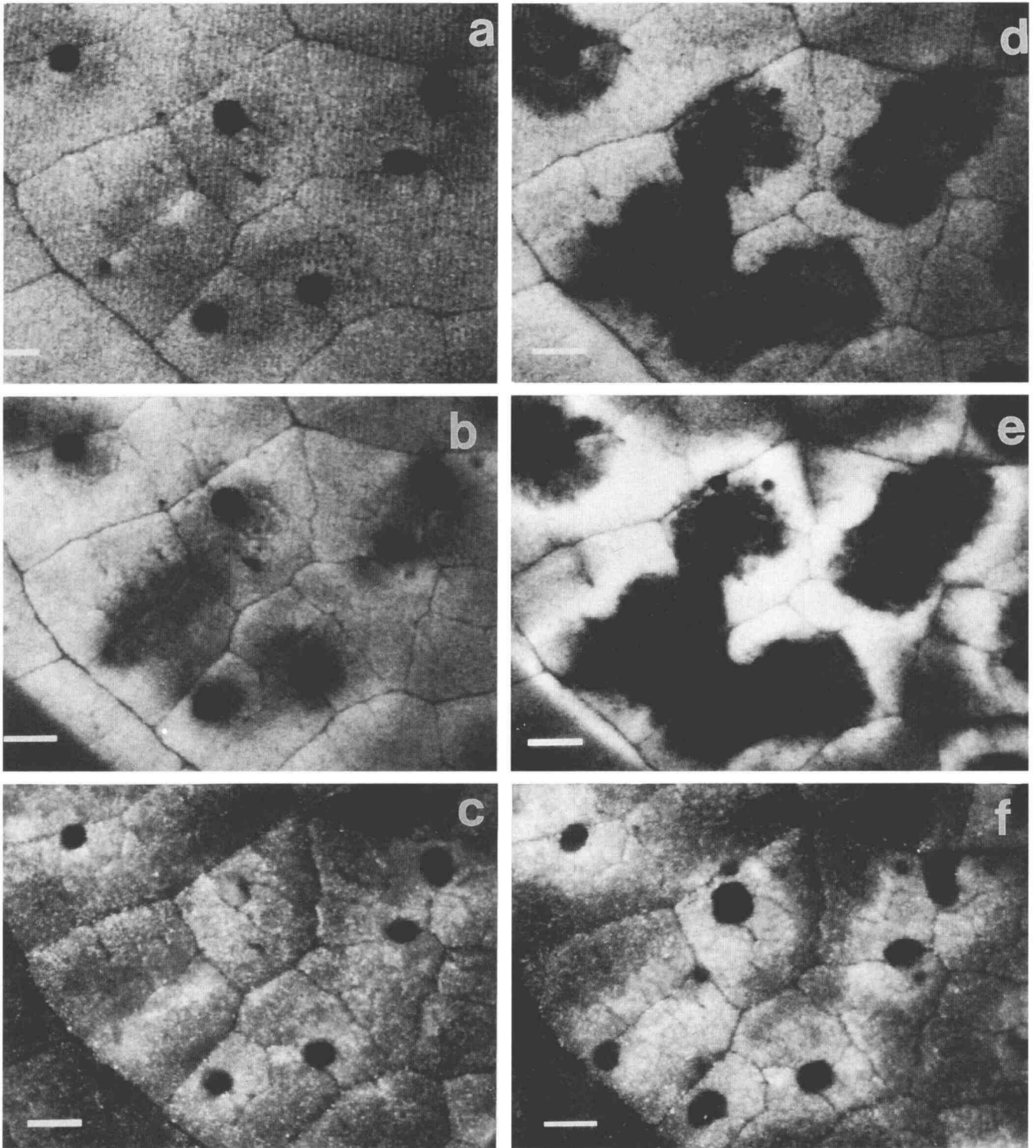
Figure 6. Images of steady-state fluorescence (a), emission at 0.6 to 1.0 s following re-illumination preceded by 5 min of darkness (b), and reflected light (c) for the leaf of Figure 4 at d 10 postinoculation. d, e, and f are the same as a, b, and c except at d 16 after inoculation.
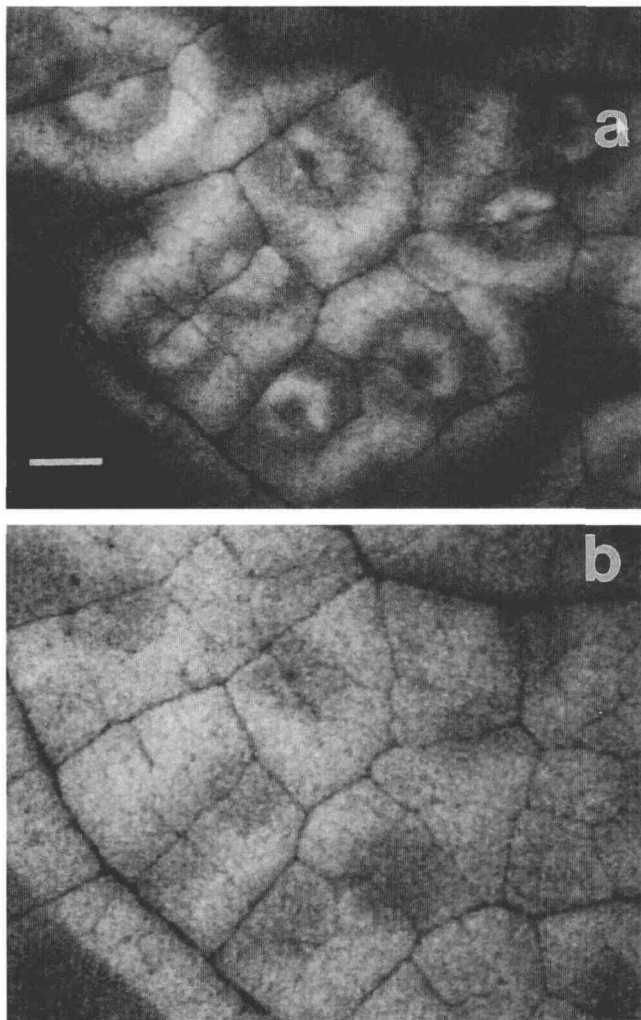
Figure 7. Images of fluorescence emission at 3 s (a) and 60 s (b) following re-illumination preceded by 5 min of darkness for the leaf of Figure 4 at d 7 after inoculation. Compare with Figure 5b.

resolution of fluorescence were used to screen for photosynthetic mutations in algal cells (Bennoun and Levine, 1967) and higher plants (Miles and Daniel, 1972). Later, imaging of the related phenomenon of delayed light emission provided evidence that leaf luminescence could provide early indications of disease or insect infestation (Björn and Forsberg, 1979). Spatial differences in fluorescence induction kinetics constitute an early response in leaves exposed to gaseous pollutants (Omasa et al., 1987). Recently, Balachandran et al. (1994a) demonstrated that a reduction in fluorescence preceded chlorosis in leaves infected with tobacco mosaic virus and measurements of fluorescence quenching were interpreted as consistent with inhibition of PSII function by the tobacco mosaic virus coat protein (Reneiro and Beachy, 1989).

In this study we showed that the increase in fluorescence to F_P in incipient lesions of bean rust was consistently higher during the early stages of infection (3–6 d). The radial increase in size of the area of enhanced fluorescence emission with time was consistent with outward growth of the mycelium from the point of invasion (Figs. 4 and 5). The kinetics of the initial fluorescence increase in infected tissue indicate that the net rate of reduction of Q_A was higher than in healthy tissue (Fig. 2). Previous work has shown that the decline in fluorescence from F_P (and, by inference the magnitude of F_P) is strongly associated with oxidation of Q_A^- during linear electron transport (Bradbury and Baker, 1981: Walker, 1981; Quick and Horton, 1984). Any decrease in the ability of the Calvin cycle to accept electrons, via NADPH, from PSI should lead to an increase in the degree of reduction of the PSI donor (P700) pool, slower oxidation of Q_A^-, and a higher fluorescence yield (Deitz et al., 1985; Peterson, 1991). This interpretation is supported by evidence that suppression of the F_S-F_M-F_T transition of the induction transient (Figs. 3b and 7b) is associated with reduced capacity for CO_2 fixation (Ireland et al., 1985). We acknowledge, however, that this view represents an oversimplification, since bean rust lesions frequently exhibit significant radial heterogeneity in fluorescence emission reflecting possibly diverse effects of infection on photosynthetic metabolism (Figs. 2a, 4b, 4d, and 7a). A similar concentric arrangement of differing physiological states has been reported for lesions on cotyledons of *Cucurbita pepo* infected with cucumber mosaic virus (Tecsi et al., 1994).

The observation of altered kinetics of fluorescence emission during induction in incipient lesions of bean rust suggests that photosynthetic capacity is affected in these areas, but the magnitude of the effect of infection on photosynthesis is not revealed by this study. Disease agents reduce photosynthesis in host tissue by a variety of means. Symptoms of water stress are commonly observed in diseased plants, e.g. *Verticillium* wilt (Bowden et al., 1990). Associated stomatal closure leads to increased nonphotochemical quenching indicative of less efficient utilization of light for photosynthesis (Daley et al., 1989; Raschke et al., 1990). Toxic substances released by the invading organism can interfere directly with electron transport, as in the case of binding of tobacco mosaic virus coat protein to PSII (Reneiro and Beachy, 1989). Likewise, key processes in photosynthetic metabolism may be affected, as evidenced by release of an inhibitor of Gln synthetase by *Pseudomonas syringae*, the agent causing wildfire disease in tobacco (Turner, 1988). Increased host-cell invertase levels were associated with imbalances in carbohydrate metabolism, resulting in feedback inhibition of photosynthesis in barley leaves infected with powdery mildew (Scholes et al., 1994).

We consider significant the fact that regions of high F_P coincide closely with sites of infection and eventual development of chlorosis in leaves. Balachandran et al. (1994b) suggested that chlorosis in response to stress and disease is a consequence of failure of photoprotective mechanisms leading to photoinhibition and photodestruction of chloroplast components. This view implies that increases in ΔpH-dependent nonphotochemical quenching, and, possibly, accumulation of the xanthophyll pigment zeaxanthin would contribute to altered patterns of light utilization in infected areas (Laasch, 1987; Demmig-Adams and Adams, 1992). Anticipated application of quantitative video-imag-

ing techniques to spatial resolution of nonphotochemical quenching with stage of disease development should enable a test of the validity of the hypothesis of Balachandran et al. (1994b) for the bean rust system.

LITERATURE CITED

Balachandran S, Osmond CB, Daley DF (1994a) Diagnosis of the earliest strain-specific interactions between tobacco mosaic virus and chloroplasts of tobacco leaves in vivo by means of chlorophyll fluorescence imaging. Plant Physiol 104: 1059–1065

Balachandran S, Osmond CB, Makino A (1994b) Effects of two strains of tobacco mosaic virus on photosynthetic characteristics and nitrogen partitioning in leaves of *Nicotiana tabacum* cv xanthi during photoacclimation under two nitrogen nutrition regimes. Plant Physiol 104: 1043–1050

Bennoun P, Levine RP (1967) Detecting mutants that have impaired photosynthesis by their increased level of fluorescence. Plant Physiol 42: 1284–1287

Björn LO, Forsberg AS (1979) Imaging by delayed light emission (phytoluminography) as a method for detecting damage to the photosynthetic system. Physiol Plant 47: 215–222

Bowden RL, Rouse DI, Sharkey TD (1990) Mechanism of photosynthesis decrease by *Verticillium dahliae* in potato. Plant Physiol 94: 1048–1055

Bradbury M, Baker NR (1981) Analysis of the slow phases of the in vivo chlorophyll fluorescence induction curve. Changes in the redox state of photosystem II electron acceptors and fluorescence emission from photosystems I and II. Biochim Biophys Acta 635: 542–551

Cardon ZG, Berry J (1992) Effects of O_2 and CO_2 concentration on the steady-state fluorescence yield of a single guard cell pair in intact leaf discs of *Tradescantia albiflora*. Plant Physiol 99: 1238–1244

Daley PF, Raschke K, Ball JT, Berry JA (1989) Topography of a photosynthetic activity of leaves obtained from video images of chlorophyll fluorescence. Plant Physiol 90: 1233–1236

Deitz K-J, Schreiber U, Heber U (1985) The relationship between the redox state of Q_A and photosynthesis in leaves at various carbon-dioxide, oxygen and light regimes. Planta 166: 219–226

Demmig-Adams B, Adams WW III (1992) Photoprotection and other responses of plant to high light stress. Annu Rev Plant Physiol Plant Mol Biol 43: 599–626

Duysens LNM, Sweers HE (1963) Mechanism of the two photochemical reactions in algae as studied by means of fluorescence. In Studies on Microalgae and Photosynthetic Bacteria. University of Tokyo Press, Tokyo, pp 353–372

Fenton JM, Crofts AR (1990) Computer aided fluorescence imaging of photosynthetic systems: application of video imaging to the study of fluorescence induction in green plants and photosynthetic bacteria. Photosynth Res 26: 59–66

Foyer C, Furbank R, Harbinson J, Horton P (1990) The mechanisms contributing to photosynthetic control of electron transport by carbon assimilation in leaves. Photosynth Res 25: 83–100

Gold RE, Mendgen K (1984) Cytology of basidiospore germination, penetration, and early colonization of *Phaseolus vulgaris* by

Uromyces appendiculatus var. *appendiculatus*. Can J Bot 62: 1989–2002

Hardham AR (1992) Cell biology of pathogenesis. Annu Rev Plant Physiol Plant Mol Biol 43: 491–526

Ireland CR, Baker NR, Long SP (1985) The role carbon dioxide and oxygen in determining chlorophyll fluorescence during leaf development. Planta 165: 477–485

Krause GH, Weis E (1991) Chlorophyll fluorescence and photosynthesis: the basics. Annu Rev Plant Physiol Plant Mol Biol 42: 313–349

Laasch H (1987) Non-photochemical quenching of chlorophyll a fluorescence in isolated chloroplasts under conditions of stressed photosynthesis. Planta 171: 220–226

Livne A (1964) Photosynthesis in healthy and rust-infected plants. Plant Physiol 64: 614–621

Livne A, Daly JM (1966) Translocation in healthy and rust-affected beans. Phytopathology 56: 170–175

Mendgen K, Deising H (1993) Tansley review no. 48. Infection structures of fungal plant pathogens—a cytological and physiological evaluation. New Phytol 124: 193–213

Miles CD, Daniel DJ (1972) A rapid screening technique for photosynthetic mutants of higher plants. Plant Sci Lett 1: 237–240

Omasa K, Shimazaki K-I, Aiga I, Larcher W, Onoe M (1987) Image analysis of chlorophyll fluorescence transients for diagnosing the photosynthetic system of attached leaves. Plant Physiol 84: 748–752

Owens TG (1995) In vivo chlorophyll fluorescence as a probe of photosynthetic physiology. In R Alscher, A Wellburn, eds, Gaseous Pollutants and Plant Metabolism. Elsevier, New York (in press)

Papageorgiou G (1975) Chlorophyll fluorescence: an intrinsic probe of photosynthesis. In Govindjee, ed, Bioenergetics of Photosynthesis. Academic Press, New York, pp 320–371

Peterson RB (1991) Effects of O_2 and CO_2 concentrations on quantum yields of photosystems I and II in tobacco leaf tissue. Plant Physiol 97: 1388–1394

Quick WP, Horton P (1984) Studies on the induction of chlorophyll fluorescence in barley protoplasts. II. Resolution of fluorescence quenching by redox state and the transthylakoid pH gradient. Proc R Soc Lond B 220: 371–382

Raschke K, Patzke J, Daley PF, Berry JA (1990) Spatial and temporal heterogeneities of photosynthesis detected through analysis of chlorophyll-fluorescence images of leaves. In M Baltscheffsky, ed, Current Research in Photosynthesis, Vol IV. Kluwer Academic, Dordrecht, The Netherlands, pp 573–578

Reneiro A, Beachy RN (1989) Reduced photosystem II activity and accumulation of viral coat protein in chloroplasts of leaves infected with tobacco mosaic virus. Plant Physiol 89: 111–116

Scholes JD, Lee PJ, Horton P, Lewis DH (1994) Invertase: understanding changes in the photosynthetic and carbohydrate metabolism of barley leaves infected with powdery mildew. New Phytol 126: 213–222

Schreiber U, Bilger W, Schliwa U (1986) Continuous recording of photochemical and non-photochemical quenching with a new type of modulation fluorometer. Photosynth Res 10: 51–62

Tecsi LI, Maule AJ, Smith AM, Leegood RC (1994) Complex, localized changes in CO_2 assimilation and starch content associated with the susceptible interaction between cucumber mosaic virus and a cucurbit host. Plant J 5: 837–847

Turner J (1988) Inhibition of photosynthesis in *Nicotiana tabacum* leaves treated with tabtoxin and its relation to pigment loss. Physiol Plant 74: 549–555

Walker DA (1981) Secondary fluorescence kinetics of spinach leaves in relation to the onset of photosynthetic carbon assimilation. Planta 153: 273–278